

ChemComm

Accepted Manuscript



This is an *Accepted Manuscript*, which has been through the Royal Society of Chemistry peer review process and has been accepted for publication.

Accepted Manuscripts are published online shortly after acceptance, before technical editing, formatting and proof reading. Using this free service, authors can make their results available to the community, in citable form, before we publish the edited article. We will replace this *Accepted Manuscript* with the edited and formatted *Advance Article* as soon as it is available.

You can find more information about *Accepted Manuscripts* in the [Information for Authors](#).

Please note that technical editing may introduce minor changes to the text and/or graphics, which may alter content. The journal's standard [Terms & Conditions](#) and the [Ethical guidelines](#) still apply. In no event shall the Royal Society of Chemistry be held responsible for any errors or omissions in this *Accepted Manuscript* or any consequences arising from the use of any information it contains.

Cite this: DOI: 10.1039/c0xx00000x

www.rsc.org/xxxxxx

ARTICLE TYPE

Polyoxometalate-Organic Supermolecular Nanotube with High Chemical Stability and Proton-Conducting Properties

Gao-Juan Cao,^{a,b} Jing-Dong Liu,^a Ting-Ting Zhuang,^a Xiu-Hong Cai,^a and Shou-Tian Zheng^{*a}

Employment of 1H-1,2,4-Triazole-3-thiol (H₂trzS) has led to a rare inorganic-organic hybrid supermolecular nanotube built from novel Ni₅-substituted polyoxotungstates, which presents interesting structural characteristics, high chemical stability, and proton-conducting properties.

Crystalline materials with molecular-based inorganic-organic hybrid tubular structures are of great interest owing to their remarkably structural peculiarities (e.g., well-defined isolated channels or pores) associated with promising applications in molecular containers/reactors, biological models, chemical recognizers, catalysis, and so on.¹⁻³ However, the development of such fascinating materials is subject to the limitation of synthetic challenges. An impressive progress in recent years is judicious choice of metal ions and organic ligands as building blocks to construct a small number of metal-organic nanotubes (MONTs).²⁻³ While, as a special kind of metal-organic frameworks (MOFs), the applications of MONTs are limited to the principal weakness of MOFs of lower chemical stability (e.g. collapse under hydrothermal conditions or in water/acidic/basic solutions).

The fabrication of materials with novel composition and topology is of particular importance because properties and applications of such materials depend on their composition and topology. In the past a few years, we participated in developing a synthetic strategy of utilizing polyoxometalates (POMs) as SBUs to substitute metal ions in MOFs for the construction of novel POM-organic frameworks (POMOFs).⁴ Compared with MOFs, POMOFs are expected to exhibit higher chemical stability because high-nuclear POM SUBs can form higher coordination numbers and thus lead to more stable skeletons. By the strategy, both extended POMOFs and zero-dimensional (0D) POM-organic cage with high hydrothermal stability have been successfully made,⁴ however, the 1D POM-organic nanotubes are still in their infancy. Up to now, though a number of POM-based tubular assemblies have been synthesized, most of them are pure inorganic, macroscale (e.g. micrometer/millimeter-sized), or non-crystalline materials.⁵ The construction of crystalline, inorganic-organic hybrid POM-organic nanotubes is greatly challenging.

Here we report a rare POM-organic supermolecular nanotube [H₂en]₄[Ni₅(OH)₃(trzS)₃(en)(H₂O)(B- α -PW₉O₃₄)]·6H₂O (**1**, en = ethylenediamine) built from previously unknown Ni₅-substituted polyoxotungstates. Unlike most MONTs with limited stability, **1** exhibits exceptional chemical and hydrothermal stability, as well as considerable thermal stability. Furthermore, AC impedance experiments reveal **1** is a kind of proton conductive material with controlled conductivity in the range from $\sim 10^{-7}$ to $\sim 10^{-4}$ S cm⁻¹.

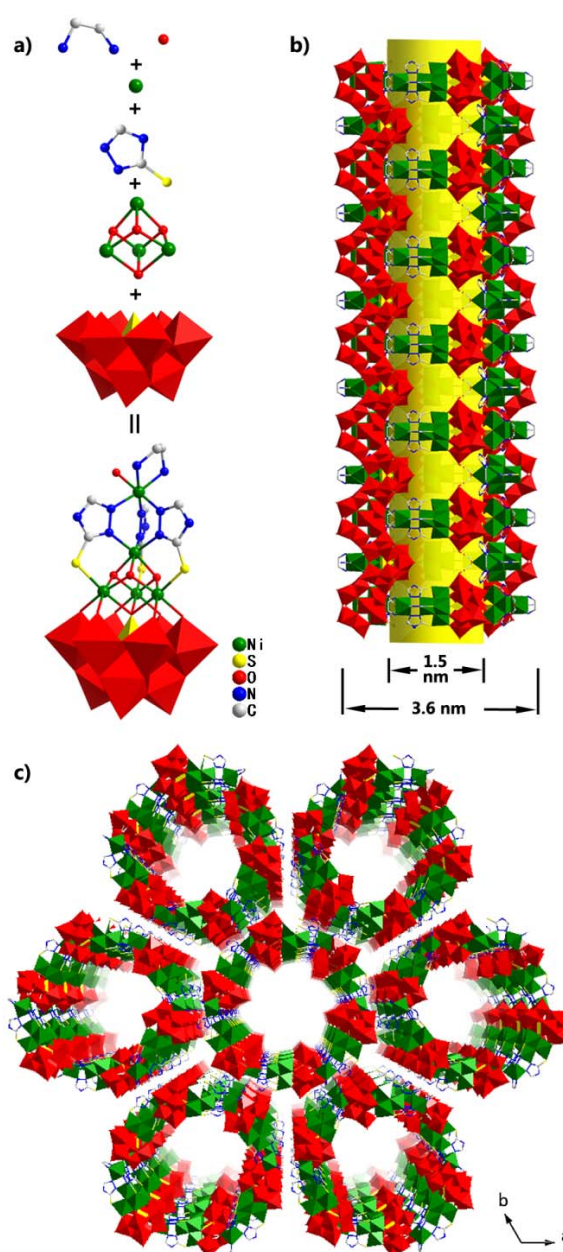


Figure 1. a) Structure **1a**; b) Side and c) top views of nanotubular structure **1**. Tungstate octahedra: red; Nickel octahedra: green.

Compound **1** crystallizes in hexagonal space group $P6_3/m$ and its structure features some intriguing characteristics. To begin with, the first introduction of a N-heterocyclic mercapto ligand

H₂trzS into POM system yielded a unique inorganic-organic hybrid Ni₅-substituted [Ni₅(OH)₃(trzS)₃(en)(H₂O)(B- α -PW₉O₃₄)]⁸⁻ (**1a**) polyoxoanion charge-balanced by four disordered protonated H₂en. As shown in Figure 1a, **1a** is a multi-component polyoxoanion and can be depicted as a multilayer assembly built from one trilacunary [B- α -PW₉O₃₄]⁹⁻ polyoxoanion, one cubane-like Ni₄O₄ core, three trzS²⁻ ligands, one Ni²⁺ ions, two terminal en ligands, and one terminal water ligand in sequence. In detail, the starting material [A- α -PW₉O₃₄]⁹⁻, which derived from a plenary { α -PW₁₂O₄₀} Keggin cluster by removal of one edge-sharing {W₃O₁₃} triad, underwent in situ isomerization during the reaction to give rise to [B- α -PW₉O₃₄]⁹⁻. Next, the polyoxoanion [B- α -PW₉O₃₄]⁹⁻ templated the formation of a cubane-like Ni₄O₄ core on its three lacunary sites. And then, one extra Ni²⁺ ion was capped to the Ni₄O₄ core through three bridging trzS²⁻ ligands, giving rise to a Ni₅-incorporated cluster {Ni₅(OH)₃(trzS)₃(B- α -PW₉O₃₄)} with idealized C_{3v} symmetry. Finally, when the remaining three coordination sites of the capping Ni²⁺ ion was further occupied by one chelated *cis*-en ligand and one water molecule, the C_{3v} symmetry was decreased to *E* due to the existences of mixed terminal ligands and the torsion angle of *cis*-en, leading to the formation of a chiral cluster **1a**.

Noteworthy, hydrothermal self-assemblies of vacant precursors {XW₉O₃₄} (X = Si, P) with Ni²⁺ ions in the presence of aliphatic amines readily form typical Ni₆-substituted inorganic-organic hybrid POMs {Ni₆(OH)₃(L)₃(XW₉O₃₄)} (L = aliphatic amine) with hexa-nuclear {Ni₆(OH)₃} cluster in a planar triangular configuration.^{4,6} The flat triangular cluster {Ni₆(OH)₃} is so stable that even the successful introductions of diverse organic ligands including carboxylic ligands and hydroxyl ligands couldn't affect its structural arrangement.^{4,6} While, the unique **1a** demonstrated that the employment of N-heterocyclic mercapto ligands to react with metal ions and POMs is a feasible way to make novel inorganic-organic hybrid POMs. It could be expected that the diversity of N-heterocyclic mercapto ligands, together with various metal ions are capable of creating a large family of novel TM-substituted POM materials.

Another important structural feature results from the inorganic-organic hybrid **1a** polyoxoanions which are elaborately joined together by multi-ply hydrogen bonds to form an intriguing hexagram-shaped supramolecular nanotube with a 3.2 nm exterior wall diameter and a 1.5 nm interior channel diameter (Figure 1b, measured between opposite atoms). A side view of the open-ended nanotube indicates the strong OH...O (2.714(11) Å) intermolecular hydrogen bonds between the terminal aqua ligands and terminal oxo atoms of {PW₉O₃₄} clusters contribute to the formation of tubular array of **1a** polyoxoanions (Figure S1). In addition, the NH...O (3.126(11) Å) interactions between the chelated en ligands and bridging oxygen atoms of {PW₉O₃₄} clusters further stabilize the tubular structure. By hydrogen bonds, every **1a** is joined to four adjacent ones, therefore the nanotube can be envisioned as a 4-connected hexagram-shaped tubular structure based on **1a** as nodes. The nanotubes are closely packed in a hexagonal manner to form an overall 3D structure **1**. An analysis using the PLATON software tool indicates that the extra-framework volumes per unit cell for **1** is 6984 Å³ (54% of the total unit cell volume).⁷

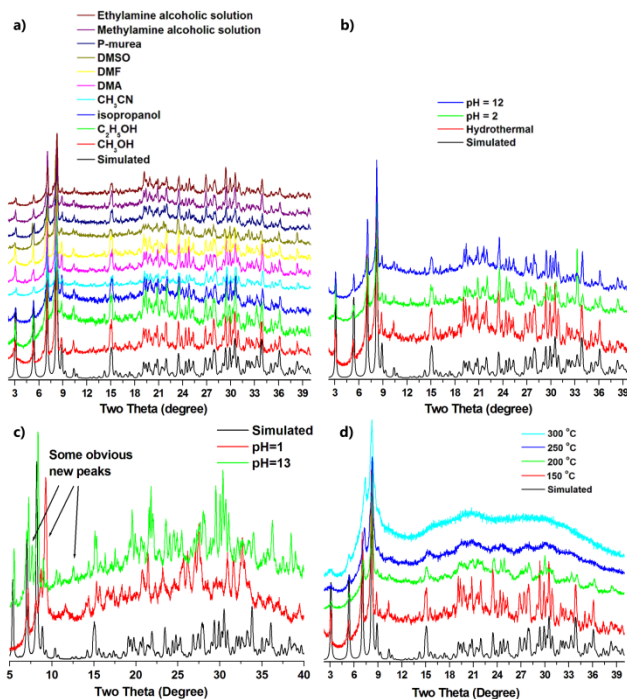


Figure 2. PXRD patterns of **1**. a) After being refluxed in different organic solvents for 48 h. b) After being hydrothermal treated at 160 °C for 48 h and soaked in water with different pH values for 48 h. c) After being soaked in water with pH = 1 or 13 for 48 h, showing there are phase transitions. d) Thermodiffractograms of the as-synthesized sample.

High structural stability (e.g. chemical, hydrothermal, and thermal stability) is key to some applications of materials. Different from MONTs that most are limited chemical stability and sensitive to moisture or water, the supermolecular nanotube **1** has exceptional stability. As shown in Figure 2, **1** exhibits a very high water-stable material so that it can remain structure even after being heated under hydrothermal conditions at 160 °C for 48 h. Additionally, **1** is also very stable in a lot of kinds of organic solvents such as CH₃OH, C₂H₅OH, isopropyl alcohol, CH₃CN, DMF, DMA, DMSO, 1,3-dimethyl-propyleneurea, methylamine and ethylamine alcoholic solutions even after being refluxed in these solvents for 48 h. Furthermore, **1** can retain its structural integrity in aqueous solution with a wide pH range from 2 to 12. Based on the PXRD data, an interesting phenomenon is found that, when the pH is adjusted to 1 or 13, **1** will undergo phase transitions to give new crystalline structures rather than structural collapse in general. Unfortunately, the structures of the new phases couldn't be determined due to their poor crystallinity. TGA of **1** showed that the removal of guest molecules occurs in the temperature range of ca. 40 - 300 °C (Figure S2), and PXRD confirmed that **1** retains its crystallinity at least up to 250 °C.

The variable temperature magnetic susceptibility of **1** was measured between 2 and 300 K (Figure S4). The $\chi_M T$ value of the **1** at 300 K is 6.67 cm³ K mol⁻¹, which are expected for the total spin-only value of five Ni²⁺ with *S* = 1 and *g* = 2.31. As the temperature decreases, the $\chi_M T$ value almost keeps stable up to about 100 K, and then start to decreases rapidly, reaching 0.77 cm³ K mol⁻¹ at 2.0 K. The temperature-dependences of $\chi_M T$ demonstrate the existence of anti-ferromagnetic coupling interaction between Ni²⁺ ions, which is different from the

ferromagnetic interactions observed in most inorganic-organic hybrid $\{XW_9O_{34}\}$ -based Ni-substituted POMs.^{4,6} The temperature dependence of the reciprocal susceptibilities ($1/\chi_m$) obeys the Curie-Weiss law above 25 K with negative $\theta = -1.43$ (Figure S5), which support the presence of overall anti-ferromagnetic coupling between the Ni^{2+} ions. The Curie constants $C = 6.11 \text{ cm}^3 \text{ mol}^{-1} \text{ K}$ are reasonable for five Ni^{2+} ions per formula.

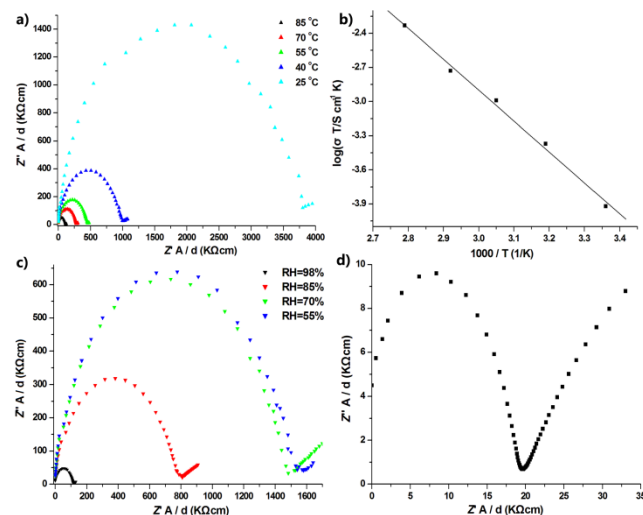


Figure 3. a) Nyquist plot for **1** under different temperatures with 98% RH. b) Arrhenius plots of the conductivity of **1**. c) Nyquist plot for **1** under different RH conditions with $T = 85 \text{ }^\circ\text{C}$. d) Impedance spectra ($85 \text{ }^\circ\text{C}$, 98% RH) of heated sample **1**.

It is noteworthy that a large quantity of pure **1** (gram-scale) can be readily prepared. The high yield, superior water stability, and the encapsulation of a lot of guests including protonated amines and H_2O within nanotube prompted us to check the proton-conducting ability of **1**. The proton conductivity was determined by ac impedance measurements using a compacted pellet of the crystalline powder sample. The bulk conductivity was evaluated by semicircle fittings of the Nyquist plots. The conductivity of **1** at 98.0% relative humidity (RH, 2 hours) and $25 \text{ }^\circ\text{C}$ is $4.0 \times 10^{-7} \text{ S cm}^{-1}$. When temperature increases from $25 \text{ }^\circ\text{C}$ to $85 \text{ }^\circ\text{C}$, the conductivity increases from 4.0×10^{-7} to $1.3 \times 10^{-5} \text{ S cm}^{-1}$ (Figure 3a). The enhanced conductivities is attributable to the raised temperature which may not only accelerate proton transition within channels, but also help the dissociation of protons from H_2en cations to water molecules to form H_3O^+ ions. The activation energy at 98% RH for the proton transfer in **1** is estimated to be 0.57 eV according to the Arrhenius equation $\sigma T = \sigma_0 \exp(-E_a/k_B T)$ (Figure 3b). Additionally, the humidity-dependent measurements at $85 \text{ }^\circ\text{C}$ show the conductivity of **1** at 55% RH is $1.0 \times 10^{-7} \text{ S cm}^{-1}$ (Figure 3c). While, when humidity is increased to 70% RH, there is a little change in the conductivity, which may be due to the absence of enough water molecules within channels. Upon increasing RH to 85%, the conductivity increases obviously and reaches $1.3 \times 10^{-5} \text{ S cm}^{-1}$ at 98% RH. Further, considering that if the encapsulated guests of en molecules are removed from channels, the material **1** might absorb more water molecules and improve its proton-conducting ability. Thus AC impedance spectroscopy on a new compacted pellet of heated crystalline powder sample (at $160 \text{ }^\circ\text{C}$ for 24 h) was performed and its result

reveals the conductivity of **1** rises up to $2.4 \times 10^{-4} \text{ S cm}^{-1}$ at 98.0% RH and $85 \text{ }^\circ\text{C}$, which is comparable to the most known proton conducting MOF materials.^{8,9}

In summary, a crystalline supermolecular nanotube **1** based on nickel-substituted POMs has been created, which is a rare type among known crystalline tubular structures. In addition, the isolation of unique Ni_5 -substituted POM in **1** opens a new route for the hydrothermal creations of novel inorganic-organic hybrid transition-metal-substituted POMs using N-heterocyclic mercapto ligands, instead of the currently popular practices that rely on aliphatic amines. Moreover, the structural stability, magnetic properties, and proton-conducting properties of **1** have been characterized, of which the remarkable hydrothermal and chemical stability would provide the opportunity for practical applications.

The work was funded by the National Natural Science Foundation of China (No. 21371033 and 21303018).

Notes and references

- ^a College of Chemistry, Fuzhou University, Fuzhou, Fujian 350108, China. E-mail: stzheng@fzu.edu.cn
- ^b Department of Applied Chemistry, College of Life Science, Fujian Agriculture and Forestry University, Fuzhou, Fujian 350002, China
- † Electronic Supplementary Information (ESI) available: Experimental details, additional characterization data, tables, and figures. See DOI: 10.1039/b000000x/
- W. L. Leong and J. J. Vittal, *Chem. Rev.*, 2011, **111**, 688; A. Carné, C. Carbonell, I. Imaz and D. Maspoch, *Chem. Soc. Rev.*, 2011, **40**, 2916; Y. Cui, Y. Yue, G. Qian and B. Chen, *Chem. Rev.*, 2012, **112**, 112; D. Wu, F. Xu, B. Sun, R. Fu, H. He and K. Matyjaszewski, *Chem. Rev.*, 2012, **112**, 3959; M. Yoon, K. Suh, S. Natarajan and K. Kim, *Angew. Chem. Int. Ed.*, 2013, **52**, 2688.
- X. L. Wang, C. Qin, E. B. Wang, Y. G. Li, Z. M. Su, L. Xu and L. Carlucci, *Angew. Chem. Int. Ed.*, 2005, **44**, 5824; T. T. Luo, H. C. Wu, Y. C. Jao, S. M. Huang, T. W. Tseng, Y. S. Wen, G. H. Lee, S. M. Peng and K. L. Lu, *Angew. Chem. Int. Ed.*, 2009, **48**, 9461; G. Yuan, C. Zhu, Y. Liu, W. Xuan and Y. Cui, *J. Am. Chem. Soc.*, 2009, **131**, 10452; Y. G. Huang, B. Mu, P. M. Schoenecker, C. G. Carson, J. R. Karra, Y. Cai and K. S. Walton, *Angew. Chem. Int. Ed.*, 2011, **50**, 436.
- X. Wang, J. Huang, S. Xiang, Y. Liu, J. Zhang, A. Eichhöfer, D. Fenske, S. Baic and C. Y. Su, *Chem. Commun.*, 2011, **47**, 3849; K. Otsubo, Y. Wakabayashi, J. Ohara, S. Yamamoto, H. Matsuzaki, H. Okamoto, K. Nitta, T. Uruga and H. Kitagawa, *Nat. Mater.*, 2011, **10**, 291; D. K. Unruh, K. Gojdas, A. Libo and T. Z. Forbes, *J. Am. Chem. Soc.*, 2013, **135**, 7398; C. R. Murdock, N. W. McNutt, D. J. Keffer and D. M. Jenkins, *J. Am. Chem. Soc.*, 2014, **136**, 671.
- S. T. Zheng, J. Zhang and G. Y. Yang, *Angew. Chem. Int. Ed.*, 2008, **47**, 3909; S. T. Zheng, J. Zhang, X. X. Li, W. H. Fang and G. Y. Yang, *J. Am. Chem. Soc.*, 2010, **132**, 15102.
- C. Ritchie1, G. J. T. Cooper, Y. F. Song, C. Streb, H. Yin, A. D. C. Parenty, D. A. MacLaren and L. Cronin, *Nat. Chem.*, 2009, **1**, 47; A. Nisar, J. Zhuang and X. Wang, *Chem. Mater.*, 2009, **21**, 3745; G. J. T. Cooper, A. G. Boulay, P. J. Kitson, C. Ritchie, C. J. Richmond, J. Thiel, D. Gabb, R. Eadie, D. L. Long and L. Cronin, *J. Am. Chem. Soc.*, 2011, **133**, 5947; Y. Shen, J. Peng, H. Pang, P. Zhang, D. Chen, C. Chen, H. Zhang, C. Meng and Z. Su, *Chem. Eur. J.*, 2011, **17**, 3657; G. J. T. Cooper, R. W. Bowman, E. P. Magennis, F. Fernandez-Trillo, C. Alexander, M. J. Padgett and L. Cronin, *Angew. Chem. Int. Ed.*, 2012, **51**, 12754; P. Huang, C. Qin, Z. M. Su, Y. Xing, X. L. Wang, K. Z. Shao, Y. Q. Lan and E. B. Wang, *J. Am. Chem. Soc.*, 2012, **134**, 14004.
- S. T. Zheng, D. Q. Yuan, H. P. Jia, J. Zhang and G. Y. Yang, *Chem. Commun.*, 2007, 1858; J. W. Zhao, J. Zhang, Y. Song, S. T. Zheng and G. Y. Yang, *Eur. J. Inorg. Chem.*, **2008**, 3809; X. X. Li, S. T.

- Zheng, W. H. Fang and G. Y. Yang, *Inorg. Chem. Commun.*, 2011, **14**, 1541; L. Huang, J. Zhang, L. Cheng and G. Y. Yang, *Chem. Commun.*, 2012, 9658; L. Yang, Y. Huo, and J. Niu, *Dalton Trans.*, 2013, **42**, 364.
- 5 7 PLATON VOIDS probe diameter 1.2 Å: A. L. Spek, *J. Appl. Crystallogr.*, 2003, **36**, 7.
- 8 J. M. Taylor, R. K. Mah, I. L. Moudrakovski, C. I. Ratcliffe, R. Vaidhyanathan and G. K. H. Shimizu, *J. Am. Chem. Soc.*, 2010, **132**, 14055; A. Shigematsu, T. Yamada, H. Kitagawa, *J. Am. Chem. Soc.*, 2011, **133**, 2034; N. C. Jeong, B. Samanta, C. Y. Lee, O. K. Farha and J. T. Hupp, *J. Am. Chem. Soc.*, 2012, **134**, 51; C. Dey, T. Kundu and R. Banerjee, *Chem. Commun.*, 2012, **48**, 266; S. C. Sahoo, T. Kundu and R. Banerjee, *J. Am. Chem. Soc.*, 2011, **133**, 17950.
- 9 T. Panda, T. Kundu and R. Banerjee, *Chem. Commun.*, 2012, **48**, 5464; G. K. H. Shimizu, J. M. Taylor and D. Kim, *Science*, 2013, 15 **341**, 354; X. Zhao, C. Mao, X. Bu and P. Feng, *Chem. Mater.*, 2014, **26**, 2492; S. S. Nagarkar, S. M. Unni, A. Sharma, K. Sreekumar and S. K. Ghosh, *Angew. Chem. Int. Ed.*, 2014, **53**, 2638.